Spectral Incoherent Solitons: A Localized Soliton Behavior in the Frequency Domain

Antonio Picozzi,[1] Stéphane Pitois,[1] and Guy Millot[1]

[1]*Institut Carnot de Bourgogne, CNRS, Université de Bourgogne, Dijon, France*

(Received 17 January 2008; published 25 August 2008)

We show both theoretically and experimentally in an optical fiber system that a noninstantaneous nonlinear environment supports the existence of spectral incoherent solitons. Contrary to conventional solitons, spectral incoherent solitons do not exhibit a confinement in the spatiotemporal domain, but exclusively in the frequency domain. The theory reveals that the causality condition inherent to the nonlinear response function is the key property underlying the existence of spectral incoherent solitons. These solitons constitute nonequilibrium stable states of the incoherent field and are shown to be robust with respect to binary collisions.

DOI: 10.1103/PhysRevLett.101.093901 PACS numbers: 42.65.Tg, 05.45.−a, 42.81.Dp

For a long time solitons have been considered as being inherently coherent localized structures and the discovery of incoherent solitons in optics has represented a significant advance in nonlinear science [1]. The incoherent soliton consists of a phenomenon of self-trapping of incoherent light in a nonlinear medium characterized by a response time τ much greater than the time correlation of the fields, $\tau \gg t_c$ [1,2]. The remarkable simplicity of the experiments realized in photorefractive materials allowed for a fruitful investigation of the dynamics of incoherent nonlinear fields [3]. It is worth noting that incoherent solitons [4] and remarkable dynamical features inherent to the incoherent nature of the fields [5,6] have also been recently investigated in instantaneous response nonlinear media.

As occurs for standard coherent solitons, incoherent solitons are characterized by a confinement of the field in the spatial or in the temporal domain [1–4]. We introduce here a novel type of incoherent solitons that are neither spatial nor temporal; i.e., the incoherent field does not exhibit any confinement in the spatiotemporal domain; however, the uncorrelated frequency components that constitute the incoherent field exhibit a localized soliton behavior in the frequency domain.

The existence of the spectral incoherent soliton relies on the property of causality of the nonlinear response function $\chi(t)$. According to linear response theory [7], the causality condition imposes restrictions on the Fourier transform of the response function $\tilde{\chi}(\omega)$, so that the real and imaginary parts of $\tilde{\chi}(\omega) = \tilde{\chi}_{\mathrm{R}}(\omega) + i\tilde{\chi}_{\mathrm{I}}(\omega)$ turn out to be related by the Kramers-Krönig relations [8]. Our theory reveals that the existence of a nonvanishing imaginary part of $\tilde{\chi}(\omega)$ is the essential property underlying the existence of spectral incoherent solitons. Indeed, the function $\tilde{\chi}_{\mathrm{I}}(\omega)$ is known to play the role of a ''gain spectrum'' for the field, which is responsible for an energy transfer from the high- to the low-frequency components of the incoherent field. Our analysis remarkably reveals that, after a transient, the averaged spectrum self-organizes in the form of a spectral soliton, which is shown to propagate without distortion in frequency space towards the low-frequency components. Moreover, the study of soliton collisions reveals that they exhibit a quasielastic interaction, thus confirming their particlelike nature.

We provide experimental evidence of the existence of spectral incoherent solitons by exploiting the natural Raman effect of conventional silica optical fibers. The Raman response function is known to exhibit complex dynamics because of the amorphous nature of silica glass [3,9]. However, by showing the existence of Raman spectral solitons, our analysis reveals that these incoherent structures are robust and can even be sustained by complicated response functions $\chi(t)$.

The existence of the spectral incoherent soliton may appear quite counterintuitive. Indeed, according to the kinetic wave theory, an incoherent field is expected to exhibit an irreversible thermalization process characterized by a H theorem of entropy growth [5,6,10]. Conversely, the causality property inherent to the response function $\chi(t)$ leads to a kinetic equation that exhibits the important property of conserving the nonequilibrium entropy. The theory then reveals that the spectral incoherent soliton constitutes a nonstationary and nonequilibrium stable state of the field, a feature of natural relevance for the important issue of fully developed turbulence. Furthermore, a kinetic equation of the same form was considered in the context of plasma physics to study Langmuir waves or stimulated Compton scattering [11], and in biological systems in the framework of the Lotka-Volterra equation [12]. In addition to random nonlinear wave systems, spectral solitons may thus find applications in the study of biochemical reactions, or in the dynamics of interacting biological species.

Let us consider the nonlinear Schrödinger (NLS) equation that takes into account a finite-time nonlinear response function $\chi(t)$,

$$i\partial_z\psi = -\beta\partial_{tt}\psi + \gamma\psi\int_{-\infty}^{+\infty}\chi(t')|\psi|^2(z, t-t')dt', \quad (1)$$

where the causality condition imposes $\chi(t) = 0$ for $t < 0$. The function $\chi(t)$ is normalized in such a way that $\int \chi dt = 1$, so that in the limit of an instantaneous response [$\chi(t) = \delta(t)$, $\delta(t)$ being the Dirac function] Eq. (1) recovers the standard NLS equation. As usual in optics, the propagation

distance z plays the role of an evolution "time" variable [3,8]. The parameter γ denotes the nonlinear coefficient and $\beta = (\partial^2 k/\partial\omega^2)/2$ the dispersion parameter [3]. In the following, we consider the highly incoherent regime of interaction in which $\epsilon = L_d/L_{\rm nl} \ll 1$, where $L_d = t_c^2/|\beta|$ and $L_{\rm nl} = 1/\gamma\langle|\psi|^2\rangle$ refer to the characteristic dispersion and nonlinear length, respectively.

A physical insight into the spectral incoherent soliton may be obtained by integrating numerically the NLS Eq. (1). The initial condition refers to a random field $\psi(z = 0, t)$ that we assume to be of *zero mean* and to obey a *stationary statistics*. In this example we consider the detailed expression of the Raman response function involved in the experiment, $\chi_0(t) = f_a h_a(t) + f_b h_b(t)$, where $h_a(t) = \tau_1(\tau_1^{-2} + \tau_2^{-2})\exp(-t/\tau_2)\sin(t/\tau_1)$, $h_b(t) = (2\tau_b - t)\exp(-t/\tau_b)/\tau_b^2$, with $\tau_1 = 12$ fs, $\tau_2 = 32$ fs, $\tau_b = 96$ fs and $f_b = 0.21$ ($f_a + f_b = 1$) [3,9]. As will be discussed later, the results we are going to present are general and do not depend on this specific form of $\chi(t)$. A typical evolution of an initial Gaussian spectrum superposed on a small-amplitude background noise is illustrated in Fig. 1(a). The simulation remarkably reveals that the spectrum splits into three components: two-soliton-like spectra (S_1, S_2) emerge from the initial condition, while the remaining energy is characterized by a small-amplitude field, which essentially evolves linearly without any significant frequency shift. The two-soliton-like spectra are shown to propagate with a constant velocity towards the low-frequency components. They are characterized by an effective width ($\Delta\omega_{\rm sol}$) of the same order than the spectral bandwidth, $\Delta\omega_{\tilde{\chi}_I} \sim \Delta\omega_{\rm sol}$ [see Fig. 2(a)]. Let us remark in Fig. 1 that the high-amplitude (i.e., high-energy) soliton S_1 is narrower and faster than the small-amplitude (i.e., low-energy) one S_2. This property has been exploited to study soliton collisions. The collision is characterized by a sudden transfer of energy that occurs from the high- to the small-energy soliton: the slow soliton is accelerated while the fast soliton is decelerated, thus revealing the existence of a quasielastic soliton interaction [Fig. 1(b)].

We underline that these numerical simulations refer to a single realization of the incoherent (stochastic) field ψ. Accordingly, the nonaveraged spectrum $|\tilde{\psi}|^2(z, \omega)$ illustrated in Fig. 1 is itself a stochastic function, which, by nature, cannot describe a genuine soliton dynamics [see the insets of Fig. 1(a) and 1(b)]. To reveal the underlying deterministic soliton behavior, one has to resort to a statistical description of the incoherent field based on an average over the realizations ($\langle\cdot\rangle$). For this purpose, the equation governing the evolution of the correlation function $B(z, \tau) = \langle\psi(z, t + \tau/2)\psi^*(z, t - \tau/2)\rangle$ can be derived by following the standard procedure based on the random-phase approximation. This approximation is known to be justified in the highly incoherent regime of interaction, $\epsilon = L_d/L_{\rm nl} \ll 1$. In this regime the statistics of the field is essentially Gaussian, so that the property of factorizability of stochastic Gaussian fields may be exploited to achieve a closure of the hierarchy of the moment's equation [10]. We follow the procedure outlined in Ref. [6], which yields [13],

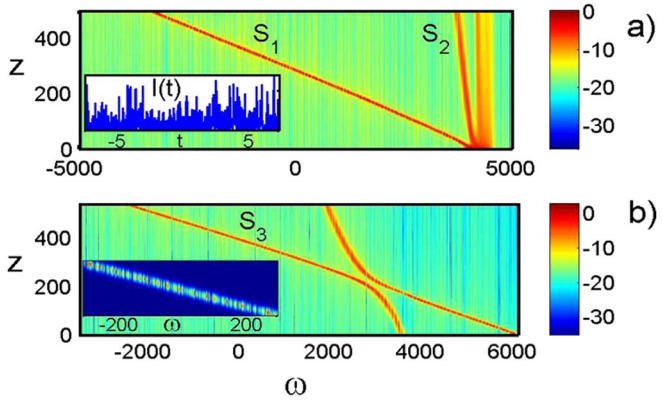

FIG. 1 (color online). Numerical simulations of the NLS Eq. (1) showing the evolution of the stochastic, i.e., nonaveraged, spectrum of the incoherent field [$|\tilde{\psi}|^2(z, \omega)$] in logarithmic scale. (a) An initial spectrum splits into two solitary-waves (S_1, S_2) and a radiationlike part; (b) the collision between such solitons reveals a quasielastic interaction [$\tau_d = (|\beta|L_{\rm nl})^{1/2} = 0.8$ ps, $L_{\rm nl} = 24$ m]. The inset in (a) shows the intensity distribution $I(t) = |\psi|^2(z, t)$ associated to S_1 at $z = 100L_{\rm nl}$: the field does not exhibit any temporal confinement. The inset in (b) shows the spectrum in normal scale. The time is in units of τ_d, ω in units of τ_d^{-1} and z in units of $L_{\rm nl}$.

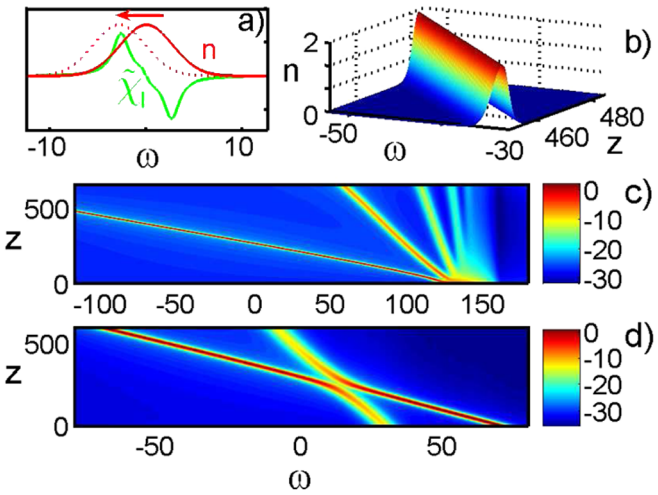

FIG. 2 (color online). (a) Schematic illustration of the soliton motion induced by the Raman spectral gain curve $\tilde{\chi}_I(\omega)$. Numerical simulations of the kinetic Eq. (2) showing the evolution of the averaged spectrum $n(z, \omega)$ of the incoherent field: (b) soliton evolution, (c) splitting of an initial broad spectrum into four solitons and a radiationlike part (logarithmic scale), (d) binary soliton collision showing an almost elastic interaction (logarithmic scale). The soliton evolution in (b) is a linear-scale plot of the high-amplitude soliton shown in (d) [z is in units of $L_{\rm nl}$, ω in units of τ_2^{-1}].

$$i\partial_z B(z,\tau) = \gamma \int_0^\infty \chi(t)[B(t)B(\tau - t) - B^*(t)B(\tau + t)]dt,$$

where "$B(t)$" stands for "$B(z, t)$" in the integrand. By Fourier transforming this equation, one obtains

$$\partial_z n(z,\omega) = \frac{\gamma}{\pi} n(z,\omega) \int_{-\infty}^{+\infty} \tilde{\chi}_{\rm I}(\omega - \omega') n(z,\omega') d\omega', \quad (2)$$

where $n(z, \omega)$ refers to the averaged spectrum of the field $[\langle \tilde{\psi}(z,\omega_1)\tilde{\psi}^*(z,\omega_2)\rangle = n(z,\omega_1)\delta(\omega_1 - \omega_2), n(z,\omega) = \int B(z,\omega)\exp(-i\omega t)dt]$. Because $\chi(t)$ is real $\tilde{\chi}_{\rm I}(\omega)$ is an odd function, which entails that Eq. (2) conserves the number of quasiparticles $\mathcal{N} = \int n d\omega$ and the nonequilibrium entropy $\mathcal{S} = \int \log[n(z,\omega)]d\omega$. This contrasts with the fundamental H-theorem of entropy growth ($d\mathcal{S}/dz \geq 0$) inherent to the kinetic wave theory [5,6,10]. Actually, the conservation of entropy in Eq. (2) originates in the causality property of the response function $\chi(t)$. This becomes apparent by remarking that Eq. (1) is almost identical to the NLS equation governing field propagation in nonlocal nonlinear media [3], provided one substitutes the response function with the nonlocal potential [$\chi(t) \rightarrow V(x)$ and $t \rightarrow x$]. The fundamental difference is that nonlocal effects are not constrained by causality. The Fourier transform $\tilde{V}(k)$ results to be purely real and Eq. (2) reduces to the trivial equation $\partial_z n(z,\omega) = 0$. Actually, the kinetic description of a nonlocal interaction requires a second-order perturbation theory in $\epsilon = L_d/L_{\rm nl}$ [6]. The corresponding kinetic equation exhibits the standard collision term that describes the expected thermalization of the field via a process of entropy production, $d\mathcal{S}/dz \geq 0$. This discussion reveals that (in the first-order approximation in ϵ) the causality property inherent to the response function $\chi(t)$ prevents the field from reaching thermal equilibrium.

The fact that Eq. (2) may exhibit solitary-wave solutions may be anticipated by remarking that, as a result of the convolution product, the spectral gain curve $\tilde{\chi}_{\rm I}(\omega)$ amplifies the front of the spectrum at the expense of its trailing edge, thus leading to a global redshift of $n(\omega)$ [see Figs. 2(a) and 2(b)]. Actually, an equation of the form (2) was considered in the context of plasma physics [11]. In the limit $\Delta\omega_{\tilde{\chi}_{\rm I}} \gg \Delta\omega_{\rm sol}$, a Gaussian-shaped solitary-wave solution was obtained through the approximation $\tilde{\chi}_{\rm I}(\omega) \propto \omega$. In the opposite limit, $\Delta\omega_{\tilde{\chi}_{\rm I}} \ll \Delta\omega_{\rm sol}$, it was pointed out that Eq. (2) reduces to a Korteg–de Vries–like equation [11]. However, our numerical study of Eq. (2) reveals that, as a rule, the width of the spontaneously generated soliton is of the same order than the gain bandwidth, $\Delta\omega_{\rm sol} \sim \Delta\omega_{\tilde{\chi}_{\rm I}}$, regardless of the details of the considered expression of $\tilde{\chi}_{\rm I}(\omega)$. Precisely, we have found numerically stable soliton solutions for various different forms of $\tilde{\chi}_{\rm I}(\omega)$, e.g., the derivative of Gaussian or of Lorentzian functions. The detailed shape of the soliton is shown to depend on the considered expression of $\tilde{\chi}_{\rm I}(\omega)$. For a given $\tilde{\chi}_{\rm I}(\omega)$, the same soliton solution may be spontaneously generated for a large class of initial conditions $n(z = 0, \omega)$. Important to note, a genuine propagation invariant solution requires a constant small-amplitude noise background [$n(\omega) \rightarrow \varepsilon$ as $|\omega| \rightarrow \pm\infty$], otherwise the soliton undergoes a slow adiabatic reshaping, so as to adapt its shape to the local value of the noise background. The numerical simulations of Eq. (2) reproduce the essential soliton properties anticipated through the analysis of the NLS Eq. (1) in Fig. 1. In particular, an initial broad spectrum is shown to split into a set of solitons and a radiationlike part [Fig. 2(c)], while the study of two-soliton collisions confirms the existence of a quasielastic soliton interaction [Fig. 2(d)].

The experiment has been realized in a silica optical fiber, whose response function is known to include an electronic quasi-instantaneous Kerr contribution and a molecular Raman contribution, $\chi_e(t) = (1 - f_R)\delta(t) + f_R\chi_0(t)$ with $f_R \simeq 0.18$ [3]. The numerical simulations of Eq. (1) reveal that, in spite of its complexity, this response function supports spectral incoherent solitons. Let us remark that, consistently with Eq. (2), spectral incoherent solitons are generated irrespective of the sign of the dispersion coefficient β [i.e., normal ($\beta > 0$) or anomalous ($\beta < 0$) dispersion], provided that $\epsilon = L_d/L_{\rm nl} \ll 1$. Conversely, for $L_d \sim L_{\rm nl}$ and $\beta < 0$, one recovers the quasicoherent regime of interaction where the standard Raman self-frequency-shift solitons are generated [3].

In our experiment we made use of a polarization maintaining (PM) optical fiber so as to guarantee that light propagates with a constant linear polarization. The incoherent wave was obtained from the amplified spontaneous emission (ASE) of a dye amplifier pumped by a Q-switched frequency-doubled Nd:YAG laser emitting 5-ns pulses at a repetition rate of 25 Hz. A spectral width as broad as $\Delta\nu \sim 20$ THz was obtained by using a DCM/SR640 dyes mixture. The central emission wavelength of the incoherent source was close to 630 nm (i.e., $\nu_0 = 475$ THz). The concentration of each dye was properly adjusted to obtain a spectrum as flat as possible over a spectral range of the same order than the Raman spectral bandwidth. Note that the pulse duration is much longer than the typical coherence time t_c, so that the incoherent source may be considered as a quasistationary statistical source. At the output of the dye amplifier, a system of half-wave plates and Glan polarizers was used to adjust the optical power and to inject the polarized ASE beam along one of the principal axes of the PM fiber.

We have first studied the evolution of the spectrum of the incoherent wave as a function of the input peak power P for different fiber lengths L [see Fig. 3(a)]. For each fiber length the mean-frequency is continuously redshifted as the power is increased. This behavior is in quantitative agreement with the numerical simulations of Eq. (1) [with $\chi(t) = \chi_e(t)$, see Fig. 3(b)], in which spectral incoherent solitons have been clearly identified. This reveals that the velocity of the soliton is not proportional to the

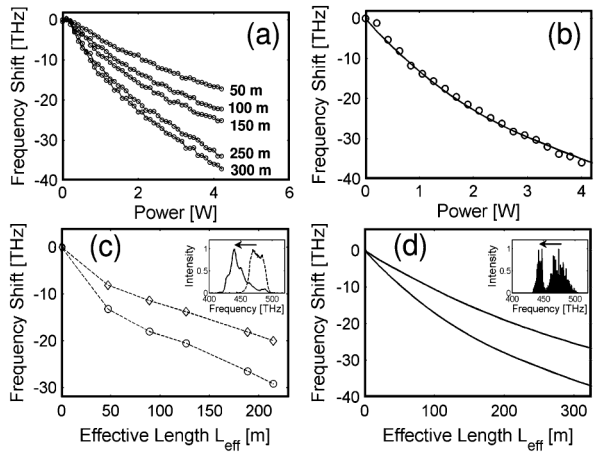

FIG. 3. (a) Experimental evolution of the mean-frequency of the spectrum of the incoherent wave vs the input peak power P for different fiber lengths L. (b) Comparison between experiment (circles) and numerical simulations of Eq. (1) (continuous line) for $L = 300$ m. (c) Experimental evolution of the mean-frequency of the spectrum vs the effective length L_{eff} for $P = 8$ W (diamonds), $P = 14$ W (circles), and corresponding numerical simulations (d). The insets represent the respective evolutions of the experimental (c) and theoretical (d) spectra: initial spectrum and the spectrum after 300 m of propagation for $P = 14$ W ($\beta = 0.03$ ps^2/m, $\gamma = 0.05$ W^{-1} m^{-1}).

power. Next, we have studied incoherent light propagation in several fiber lengths L. Figure 3(c) represents the evolution of the mean-frequency vs the propagation distance for two different input powers. To take into account linear fiber losses ($\alpha = 2.3$ km^{-1}), we have represented the evolution of the frequency shift in terms of the effective length, defined as $L_{\text{eff}} = [1 - \exp(-\alpha L)]/\alpha$ [3]. After a transient stage, the frequency shift exhibits a monotonic variation which is almost proportional to the propagation distance, in agreement with the properties of the spectral incoherent soliton [Figs. 1, 2, and 3(d)]. Note that the lines in Figs. 3(c) and 3(d) exhibit a small curvature, a feature that could be ascribed to the fact that the mean-frequency has been calculated from the whole spectrum, and thus includes the ''nonsolitonic radiationlike'' part. This point is illustrated in the inset of Fig. 3(c), which represents the incoherent spectrum at the fiber input (dashed line) and after 300 m of propagation (solid line). We clearly observe the formation of a spectral peak that is continuously shifted away from the radiationlike part of the spectrum.

In summary, we have reported theoretically and experimentally incoherent structures whose soliton behavior manifests itself exclusively in the frequency domain. The spectral soliton is sustained by the combined effects of dispersion and nonlinearity: in the absence of dispersion the spectrum would be highly deformed, while in the absence of nonlinearity the spectrum would not evolve at all. These incoherent structures may thus be expected to arise in any radiation-matter interaction whose finite-time response could not be neglected. Spectral incoherent solitons are also relevant to many branches of nonlinear physics owing to the universality of the NLS equation. Furthermore, note that the discretized version of the kinetic Eq. (2) takes the following form, $\partial_t n_i = n_i \sum_j \chi_{ij} n_j$, with $\chi_{ij} = -\chi_{ji}$. This equation recovers the structure of the generalized Lotka-Volterra equation, which is known to provide a generic description of biochemical population dynamics [12], $n_j(t)$ referring to the temporal evolution of the population of the jth species (or the jth chemical reacting component). In this context, the spectral soliton manifests itself as a dynamical birth-death process, in which novel species are continuously regenerated in the front of the soliton, while they disappear at its trailing edge; i.e., the populations of new species grow up absorbing species previously generated until they are aborbed in turn by the newly generated species.

This work has been supported by the Agence Nationale de la Recherche (ANR).

[1] M. Mitchell *et al.*, Phys. Rev. Lett. **77**, 490 (1996); M. Segev and D. N. Christodoulides, *Incoherent Solitons*, edited by S. Trillo and W. Torruellas, Spatial Solitons (Springer, Berlin, 2001).
[2] See, e.g., D. N. Christodoulides *et al.*, Phys. Rev. Lett. **78**, 646 (1997); N. N. Akhmediev and A. Ankiewicz, Phys. Rev. Lett. **83**, 4736 (1999); M. Peccianti and G. Assanto, Opt. Lett. **26**, 1791 (2001); S. A. Ponomarenko and G. P. Agrawal, Phys. Rev. E **69**, 036604 (2004); O. Bang, D. Edmundson, and W. Krolikowski, Phys. Rev. Lett. **83**, 5479 (1999).
[3] Y. S. Kivshar and G. P. Agrawal, *Optical Solitons: From Fibers to Photonic Crystals* (Academic, New York, 2003).
[4] A. Picozzi and M. Haelterman, Phys. Rev. Lett. **86**, 2010 (2001); Phys. Rev. Lett. **92**, 143906 (2004); M. Wu *et al.*, Phys. Rev. Lett. **96**, 227202 (2006); O. Cohen *et al.*, Phys. Rev. E **73**, 015601 (2006).
[5] C. Connaughton *et al.*, Phys. Rev. Lett. **95**, 263901 (2005); S. Pitois, S. Lagrange, H. R. Jauslin and A. Picozzi, Phys. Rev. Lett. **97**, 033902 (2006); S. Lagrange, H. R. Jauslin, and A. Picozzi, Europhys. Lett. **79**, 64 001 (2007).
[6] See, e.g., A. Picozzi, Opt. Express **15**, 9063 (2007).
[7] M. Le Bellac *et al.*, *Equilibrium and Nonequilibrium Statistical Thermodynamics* (Cambridge University Press, Cambridge, England, 2004).
[8] R. W. Boyd, *Nonlinear Optics* (Academic, New York, 2002).
[9] Q. Lin and G. P. Agrawal, Opt. Lett. **31**, 3086 (2006).
[10] V. E. Zakharov, V. S. L'vov, and G. Falkovich, *Kolmogorov Spectra of Turbulence I* (Springer, Berlin, 1992).
[11] Ya. Zel'dovich *et al.*, Sov. Phys. JETP **35**, 733 (1972); S. L. Musher, A. M. Rubenchik, and V. E. Zakharov, Phys. Rep. **252**, 177 (1995).
[12] N. S. Goel *et al.*, Rev. Mod. Phys. **43**, 231 (1971).
[13] We made use of Eq. (1) and $\langle \psi(t_1)\psi^*(t_2)\psi(t_2 - t')\psi^*(t_2 - t')\rangle = B(\tau)B(0) + B(\tau + t')B^*(t')$.